Check for updates

Insights into sustainable aerogels from lignocellulosic materials

Hoang S. H. Nguyen, [ID] *[a] Ha Ky Phuong Huynh, [ID] [bd] Son Truong Nguyen,[bcd] Van T. T. Nguyen,[e] Tuan-Anh Nguyen[bd] and Anh N. Phan*[a]

Aerogels, the three-dimensional materials, have been considered to be revolutionary solid-state materials due to their highly porous structure, low density, large surface area, and low thermal conductivity, which can be applied in the many modern fields of industry. Since its discovery in 1931, research related to aerogels has expanded from the exploration of starting materials to synthesis routes and applications (*e.g.*, thermal, sound insulation materials, and wastewater treatment). The limitations of conventional aerogels (silica, resorcinol/formaldehyde), which are unsustainable, non-biodegradable, and expensive materials has motivated researchers to seek alternative materials. In this regard, lignocellulose is a better candidate and thus has attracted the attention of the community. This review critically analyzes the current state-of-the-art in aerogel synthesis from lignocellulosic components and the entire lignocellulose biomass, focusing on the effects of synthesis routes and conditions on aerogel properties. Perspectives on pre-treatment, synthesis approaches, potential applications, and future development will be discussed.

1 Introduction

Aerogels are solid materials with unique properties such as high porosity (90–99%), low density (0.001–0.5 g cm^{-3}), large specific surface area (up to 2000 m^2 g^{-1}), and low thermal conductivity (0.01–0.04 W m^{-1} K^{-1}).[1,2] These excellent properties make aerogels ideal as thermal insulation materials,[3–5] catalyst supports,[6–8] and adsorbents for wastewater treatment.[9–11]

In terms of classification, aerogels are classified as inorganic aerogels (*e.g.*, SiO$_2$ (ref. 12 and 13)) or organic aerogels (*e.g.*, resorcinol/formaldehyde (RF) and melamine/formaldehyde (MF)[14]). Organic aerogels could be further divided into non-biodegradable synthetic polymers (*e.g.*, polyvinyl alcohol (PVA), polyurethane (PU)) and biodegradable natural polymers or biopolymers (*e.g.*, cellulose).[15] One class of inorganic aerogels is carbon aerogels, which are fabricated by pyrolyzing organic aerogels.[16]

Aerogels are synthesized by following three consecutive steps: (1) gelation and ageing, (2) solvent exchange, and (3) drying. In the first stage, colloidal particles dispersed in a solution link together *via* hydrolysis and/or polycondensation to create a 3D solid network whose pores are filled with liquid (wet gel) as a result of the polymerization process by mixing over a period of time.[17] This step is crucial to determining the structure of aerogels. The gel skeleton is then reinforced in the ageing step by controlling the temperature and time.[12,17] In the second stage, the initial solvent in the gel is exchanged with a lower surface tension solvent to minimize the shrinkage and collapse of the aerogel during the drying stage.[18,19] The final drying step is considered the most critical step in the preparation of aerogel with a minimum damage of capillary stresses to the gel network to maintain the pore structure of the aerogel.[19,20]

Recently, there has been a growing interest in using biopolymers present in lignocellulose to synthesize aerogels (often referred to as bio-based aerogels) because they not only possess excellent properties, such as highly porous, low density, low thermal conductivity (TC) and toxicity, but are also green, biodegradable,[21] and inexpensive due to their abundance. In general, a fundamental difference between bio-based aerogels and conventional aerogels is that conventional aerogels (*e.g.*, silica, RF, and MF) start with monomers, hence require a polymerisation step to form polymers. In contrast, cellulose, hemicellulose, and lignin are "ready" polymers, which do not require the polymerisation step but there is an arrangement of polymer chains *via* dissolution or dispersion. All three polymers in lignocellulose have been proven for possible use in aerogel preparation.[22–24]

[a]School of Engineering, Newcastle University, NE1 7RU, UK. E-mail: hoang.nguyen@newcastle.ac.uk; anh.phan@newcastle.ac.uk

[b]Faculty of Chemical Engineering, Ho Chi Minh City University of Technology (HCMUT), 268 Ly Thuong Kiet St., Dist. 10, Ho Chi Minh City, Vietnam

[c]Research Institute for Sustainable Energy, Ho Chi Minh City University of Technology (HCMUT), 268 Ly Thuong Kiet St., Dist. 10, Ho Chi Minh City, Vietnam

[d]Vietnam National University Ho Chi Minh City, Linh Trung Ward, Thu Duc Dist., Ho Chi Minh City, Vietnam

[e]Institute of Chemical Technology, Vietnam Academy of Science and Technology, Dist. 12, Ho Chi Minh City, Vietnam

This journal is © The Royal Society of Chemistry 2022

J. Mater. Chem. A, 2022, **10**, 23467–23482 | **23467**

Although a number of review articles have been published discussing the properties, synthesis approaches, and applications of cellulose-based aerogels[1,25] and lignin-based aerogels,[23] these reviews have mainly focused on individual polymers fractionated from biomass. This review will focus on aerogels from individual components (cellulose, hemicellulose, and lignin) and the entire lignocellulose biomass. We will systematically analyze and critically discuss current developments in their synthesis. Parameters affecting aerogel properties will be analyzed and discussed. This review is expected to provide useful information for the optimization and offer guidance in choosing the materials and synthesis route if a certain application is identified. Furthermore, current challenges in aerogel production and future perspectives of developing the aerogel synthesis process from lignocellulosic materials will be discussed in detail.

2 Current development of aerogels from lignocellulosic materials

2.1 Cellulose-based aerogels

Cellulose, the most common component from lignocellulose, is used to prepare aerogels because of its availability and its aerogel properties (*e.g.*, larger surface area (SA), higher porosity) compared to lignin and hemicellulose aerogels.[22] Cellulose aerogels can be synthesized by two methods: (a) dispersion or (b) dissolution, as illustrated in Fig. 1. The former involves the uniform dispersion of cellulose fibers in water, whereas the latter involves dissolved cellulose fibers in a solution (*e.g.*, NaOH, ionic liquids).[1,25] Cellulose aerogels not only exhibit high porosity (92–99%), and low density (0.015–0.1 g cm^{-3}), which are comparable to those of silica or synthetic polymer aerogels, but also have better biodegradability and higher compressive strength (*e.g.*, 5.2–16.67 kPa for cellulose aerogels compared to 0.5–1 kPa for silica aerogels).[1]

In the dispersion route (Fig. 1a), cellulose fibers are dispersed in deionized water in the presence of cross-linkers (*e.g.* polyvinyl alcohol (PVA)[28] or Kymene[29]) to cross-link cellulose molecules. The hydrogen bonds between the hydroxyl groups of cellulose and PVA are formed at the curing step. Based on these linkages, the porous structure of the aerogel is formed and maintained after drying step.[5] The aerogels prepared *via* the dispersion route are highly porous (the porosity range of 96–98% (ref. 5 and 28–30)). As a result, aerogels have low thermal conductivity of 0.025–0.04 W m^{-1} K^{-1},[5,9,28,31] which is comparable to silica aerogels (0.026 W m^{-1} K^{-1}), wool (0.03–0.04 W m^{-1} K^{-1}).[28] Increasing the concentration of cellulose fibers leads to a denser structure and decreases the pore size of aerogels, thereby minimizing the sound transmitting through the aerogel, thus the noise reduction coefficient increases.[28]

The second route to obtain cellulose aerogels is *via* dissolution (Fig. 1b), which cleaves the hydrogen bonds between
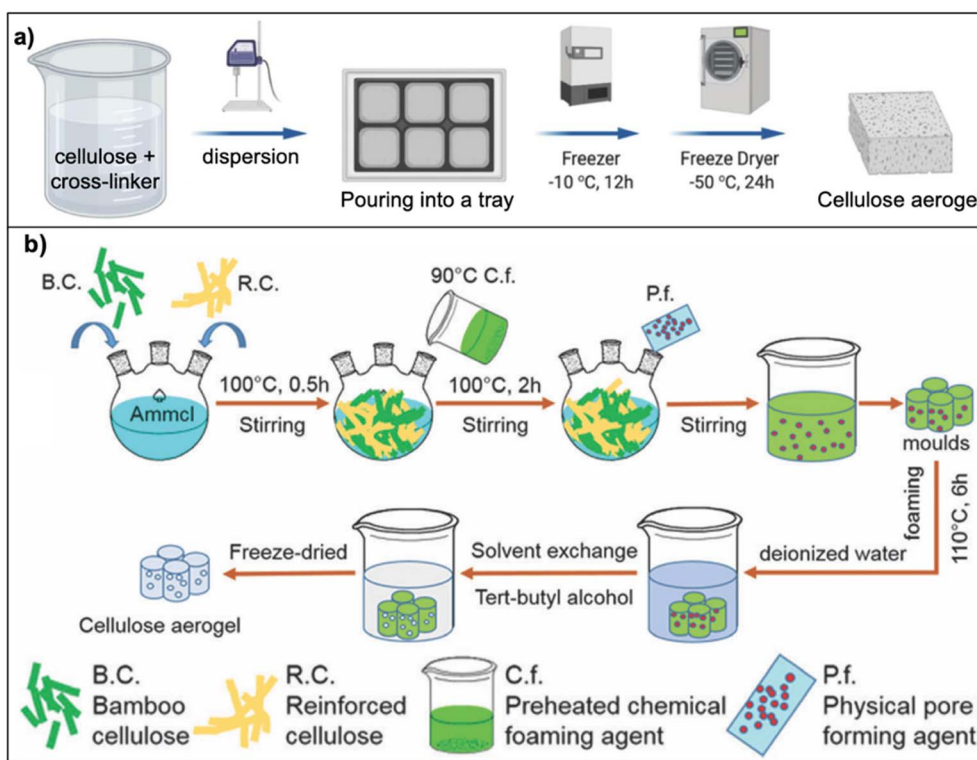

Fig. 1 Schematic preparation of cellulose aerogels: (a) dispersion route ref. [26] (Adapted from Duong, H. M., Ling, N. R. B., Thai, Q. B., Le, D. K., Nguyen, P. T. T., Goh, X. Y. and Phan-Thien, N., A novel aerogel from thermal power plant waste for thermal and acoustic insulation applications, *Waste Management*, **124**, 2021, 1–7, copyright 2021, with permission from Elsevier), (b) dissolution route (reproduced from ref. [27] with permission from PCCP Owner Societies).

23468 | *J. Mater. Chem. A*, 2022, **10**, 23467–23482

This journal is © The Royal Society of Chemistry 2022

cellulose molecules by ionic liquids (IL) or NaOH. Then, the dissolved gel is regenerated by an anti-solvent (e.g., water, methanol, or ethanol), by which the intramolecular and inter-molecular bonds between cellulosic chains are reformed.[25] For instance, when ionic liquid 1-butyl-3-methyl imidazolium chloride is used to dissolve cellulose,[32] oxygen and hydrogen atoms of cellulose form electron donor–electron acceptor (DEA) complexes with the charged species of IL. This interaction leads to the separation of hydroxyl groups of different cellulosic chains.[33] Several ILs have been used as dissolution solvents, such as 1-butyl-3-methylimidazolium chloride (BmimCl),[32] 1-allyl-3-methylimidazolium chloride/dimethyl sulfoxide (AmimCl/DMSO) co-solvent system.[34] The resultant aerogels have a comparable porosity to those obtained from the dispersion route (ranging from 96–99%) as shown in Table 1. However, there is a significant difference in SA, specifically, 28–102 m^2 g^{-1} for cotton stalks in AmimCl/DMSO co-solvent system[34] and 186 m^2 g^{-1} for microcrystalline cellulose in BmimCl.[32] It can be explained due to the differences in properties of the starting materials, synthetic route, and synthetic conditions. It was reported[34] that pure cellulose results in better aerogel properties (e.g., larger SA) than lignocellulose containing other compounds such as lignin and hemicellulose. Aatonen and Jauhiainen (2009) synthesized aerogels from cellulose, hemicellulose, lignin, and a synthetic lignocellulose solution using ionic liquid BmimCl and found that pure cellulose produced an aerogel with the largest SA of 539 m^2 g^{-1}, whereas cellulose aerogels with impurities (lignin, hemicellulose) had SA in the range of 120–210 m^2 g^{-1}.[22] Further discussion regarding aerogels from the whole lignocellulose biomass will be given in Section 2.3.

In the dissolution process of cellulose using NaOH/water,[35] OH^- will cleave the hydrogen bonds, and Na^+ stabilizes the hydrophilic parts of cellulose. Urea could be also added (e.g., NaOH/urea[36]) to improve the solubility of cellulose in the solution by stabilizing the hydrophobic parts of cellulose, thus preventing cellulose molecules from re-aggregating.[37] The properties of aerogels prepared via dissolution in NaOH are comparable to those in IL, as shown in Table 1. However, IL dissolves cellulose in a wide range of concentrations and molecular masses,[24] especially high DP cellulose (DP > 250 (ref. 38)), which will be easier to form the gel, and it will be more stable compared to NaOH, which can dissolve cellulose at DP < 200 (ref. 39) and the solution is not stable and easy to form gel.[37]

Table 1 Summary of aerogels obtained from cellulose derived from biomass[a]

Material	Synthetic route	Properties	Applications	Ref.
Pineapple leaves and cotton waste	Dispersion	Porosity: 96% Density: 0.019–0.046 g cm^{-3} TC: 0.039–0.043 W m^{-1} K^{-1}	Heat insulation	5
Sugarcane bagasse	Dispersion	Porosity: 92–99% Density: 0.016–0.112 g cm^{-3} TC: 0.031–0.042 W m^{-1} K^{-1}	Oil removal	9
Pineapple leaves	Dispersion	Porosity: 99% Density: 0.013–0.033 g cm^{-3} TC: 0.030–0.034 W m^{-1} K^{-1} SA: 3.65–7.32 m^2 g^{-1}	Heat and sound insulation oil removal	28 and 40
Pineapple leaves and activated carbon	Dispersion	Porosity: 91–96% Density: 0.032–0.093 g cm^{-3}	Ethylene gas adsorption and Ni(II) removal	30
Spent coffee grounds and cotton pads	Dispersion	Porosity: 92–95% Density: 0.013–0.033 g cm^{-3} TC: 0.037–0.045 W m^{-1} K^{-1}	Oil removal	41
Wood pulp	Dispersion	Density: 0.058 g cm^{-3} SA: 22.4 m^2 g^{-1}	Flame retardant	42
Natural pine needles	Dispersion	Density: 0.031 g cm^{-3} SA: 20 m^2 g^{-1}	No demonstration (n.d.)	43
Native cellulose	Dissolution in NaOH	Porosity: 91–95% Density: 0.06–0.3 g cm^{-3} SA: 200–300 m^2 g^{-1}	n.d.	35
Paper waste	Dissolution in NaOH/urea	Porosity: 97% Density: 0.04 g cm^{-3}	Oil removal	36
Cellulose	Dissolution in NaOH/urea	Porosity: 85–98% Density: 0.01–0.4 g cm^{-3}	n.d.	44
Cotton liner pulp	Dissolution in IL	Porosity: 86–90% Density: 0.01–0.06 g cm^{-3}	Adsorption of bovine serum albumin	45
Microcrystalline cellulose	Dissolution in IL	Porosity: 99% SA: 186 m^2 g^{-1}	n.d.	32
Cotton stalks	Dissolution in IL	Porosity: 96–98% Density: 0.1–0.15 g cm^{-3} SA: 28–102 m^2 g^{-1}	n.d.	34

[a] SA is surface area, TC is thermal conductivity, IL is an ionic liquid, n.d. is no demonstration.

This journal is © The Royal Society of Chemistry 2022

J. Mater. Chem. A, 2022, 10, 23467–23482 | 23469

Although aerogels prepared by dispersion and dissolution methods have nearly similar porosity, ranging from 91–99% (Table 1), there is an obvious difference in fiber diameters, in that, the dissolution route produces thinner fibers than in the dispersion route, as shown in Fig. 2. The size of the fibers affects the SA of aerogels. Aerogels synthesized *via* the dispersion route had an SA of 25 m^2 g^{-1}, much smaller than those of aerogels prepared by the dissolution route (300 m^2 g^{-1}) (Table 1). It could be because large-diameter fibers promote agglomeration, leading to a lower pore volume and therefore reducing SA.[46] The dissolution route produces aerogels with smaller pore sizes, leading to a larger SA. Cellulose aerogels synthesized *via* the dispersion route (Fig. 2c and d) have cellulose fibers muddled together. In contrast, cellulose aerogels prepared *via* the dissolution route have thinner fibers that are more uniform and arranged into a 3D-web-like structure (Fig. 2a and b). Although the regenerated cellulose aerogels prepared *via* the dissolution–regeneration route have better properties than those prepared by the dispersion route, the regenerated aerogels require multiple steps, such as the removal of dissolution solvent and solvent exchange. For the dispersion method, there is no requirement for a solvent exchange step. However, the uniform-dispersion step of cellulose is crucial and this strongly depends upon synthetic conditions, such as cellulose fiber concentration, mixing, cross-linking type, concentration, time, and temperature. The effects of these parameters, however, have not been fully examined.

Researchers have considered hybridizing different materials with cellulose fibers to produce composite aerogels to improve properties, for instance, cellulose nanocrystals and red mud[47] to improve magnetic conductivity, surface area or spent coffee ground and cotton pads[41] to improve oil adsorption capacity and compressive Young's modulus. Even though the properties of hybrid aerogels normally show significant improvement over non-hybrid aerogels, there is still a gap in the fundamental and theoretical basis of the tunability of interactions between cellulose and other materials. Further understanding is needed that will allow researchers to expand the functionality of these systems in a systematic way. Rahmanian and co-workers published a review of cellulose-based hybrid aerogels, covering different aspects such as fabrication approach, application, and types of hybrid aerogels (*e.g.*, with silica, graphene or graphene oxide, metal–organic framework).[48] To avoid repetition, the reader is encouraged to refer to ref. [48] for further details.

2.2 Lignin- and hemicellulose-based aerogels

Lignin, sharing up to 25% of lignocellulosic materials, contains phenolic polymer precursors such as macromolecules *p*-coumaryl alcohol, coniferyl alcohol, and sinapyl alcohol, which
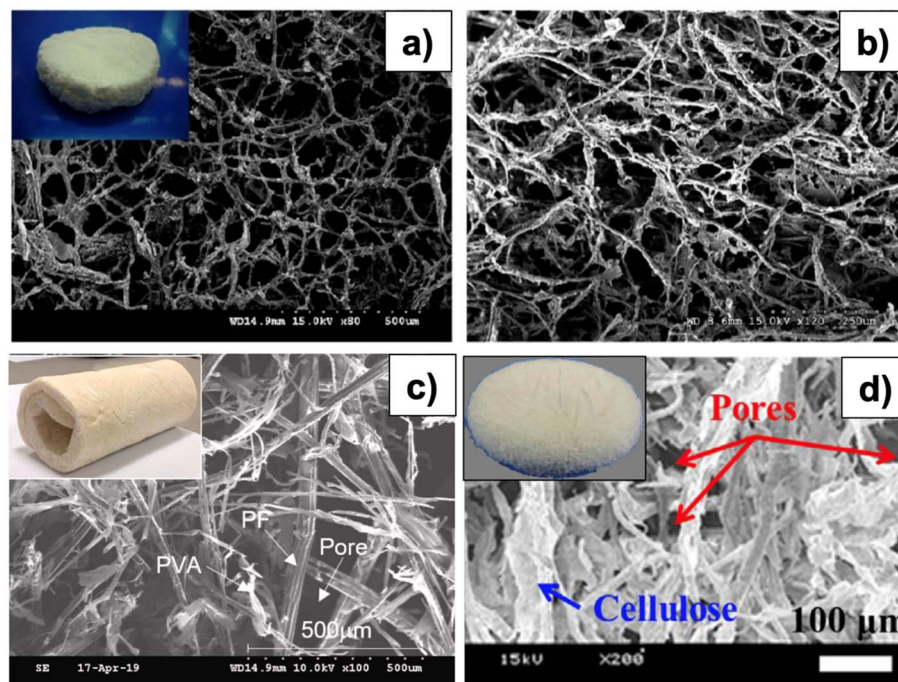

Fig. 2 SEM images of (a) before and (b) after coating methyltrimethoxysilane (MTMS) from recycled paper waste aerogels (Reprinted with permission from Nguyen, S. T., Feng, J., Le, N. T., Le, A. T. T., Hoang, N., Tan, V. B. C. and Duong, H. M., Cellulose Aerogel from Paper Waste for Crude Oil Spill Cleaning, *Industrial & Engineering Chemistry Research*, 2013, **52**, 18386–18391.[36] Copyright (2013) American Chemistry Society), (c) from Pineapple Aerogel,[28] (Adapted from Do, N. H. N., Luu, T. P., Thai, Q. B., Le, D. K., Chau, N. D. Q., Nguyen, S. T., Le, P. K., Phan-Thien, N. and Duong, H. M., Heat and sound insulation applications of pineapple aerogels from pineapple waste, *Materials Chemistry and Physics*, 2020, **242**, 122267, copyright 2020, with permission Elsevier), (d) from recycled cellulose fibers[29] (Adapted from Feng, J., Nguyen, S. T., Fan, Z. and Duong, H. M., Advanced fabrication, and oil absorption properties of super-hydrophobic recycled cellulose aerogels, *Chemical Engineering Journal*, 2015, **270**, 168–175, copyright 2015, with permission from Elsevier). Top row: aerogels prepared by the dissolution route, bottom row: aerogels prepared by the dispersion route.

23470 | *J. Mater. Chem. A*, 2022, **10**, 23467–23482

This journal is © The Royal Society of Chemistry 2022

correspond to *p*-hydroxyphenyl, guaiacyl, and syringyl monomer units.[49] Resorcinol/formaldehyde (RF) aerogel is the most studied organic aerogel, but the high cost of resorcinol hinders RF from mass production. Chen *et at.* reported that lignin could substitute resorcinol to prepare lignin-resorcinol-formaldehyde (LRF) aerogels that had SA in a range of 191–478 $m^2 g^{-1}$, large mesopore volume (V_{mes} = 0.834–0.895 $cm^3 g^{-1}$),[50] which was comparable to an aerogel prepared from resorcinol (SA = 552 $m^2 g^{-1}$, V_{mes} = 0.895 $cm^3 g^{-1}$). Increasing the lignin content increases the pore width and decreases the pore volume, leading to a smaller SA.[50] The amount of phenolic precursors in lignin also affected aerogels' properties *e.g.*, kraft lignin-based carbon aerogel had a larger SA of 121 $m^2 g^{-1}$ than an organosolv lignin-based carbon aerogel (20 $m^2 g^{-1}$) because the kraft lignin has more reaction sites (*p*-coumaryl alcohol and coniferyl alcohol) with formaldehyde than organosolv lignin.[51] Experimental conditions, such as the ratio of lignin to formaldehyde, temperature, mixing, and reaction time also influence the properties of the prepared aerogel. For instance, a higher ratio of formaldehyde to lignin resulted in lower SA of aerogels, while the opposite effect was observed in carbon aerogels, in that, SA increased with an increase in the formaldehyde to lignin (F/L) ratio (Fig. 3). This can be explained because side reactions of formaldehyde during the synthesis produced compounds such as polyoxymethylene or paraformaldehyde occupying the pores of the aerogels. Therefore, the higher the amount of formaldehyde, the more pores are occupied, therefore reducing the pore volume and SA (see Fig. 3). When aerogels are carbonized, those compounds are decomposed into gases, leading to the formation of additional pores, which shrink, generating smaller pores and larger SA.[52] However, other synthetic conditions such as temperature, mixing, and reaction time have not been studied.

To date, cellulose aerogel has been the focus, and lignin has been considered an unwanted by-product in the pre-treatment and preparation steps. However, a pre-treatment and fractionation of lignocellulose to obtain lignin-free cellulose require the use of harsh chemicals and severe conditions,[9,43] resulting in waste treatment problems, thus increasing operational costs. Prior studies showed[53] that the incorporation of lignin could enhance certain properties of cellulose-based materials, such as hydrophobicity. Therefore, utilizing the 'already' present lignin in lignocellulose to produce cellulose aerogels would not only reduce the use of chemicals but also give aerogels better properties. Nonetheless, the presence of lignin might interfere with hydrogen bonding between cellulose fibrils, hence weakening bonds and reducing mechanical properties.[53] However, there is still little evidence and understanding of how lignin interacts with cellulose molecules during the preparation of aerogels to enhance or degrade the properties of aerogels.

Aerogels from pure hemicellulose are scarce with little information about their properties.[54] Instead, hemicellulose is normally coupled with other polymers, such as cellulose and lignin to prepare aerogels. It was reported[22] that an aerogel with a small amount of hemicellulose (cellulose : hemicellulose : lignin = 2 : 0.7 : 1) had a lower SA (213 $m^2 g^{-1}$) and higher density (d = 0.114 $g cm^{-3}$) than a pure cellulose aerogel (SA = 539 m^2 g, d = 0.048 $g cm^{-3}$). Therefore, further research on the effect of hemicellulose and its derivatives on cellulose aerogel is needed so that a suitable pre-treatment/fractionation can be applied to obtain the required properties of starting materials for aerogels. Interactions between the properties of the starting materials and synthetic conditions should be focused on to develop an efficient process to produce aerogels from lignocellulosic materials.
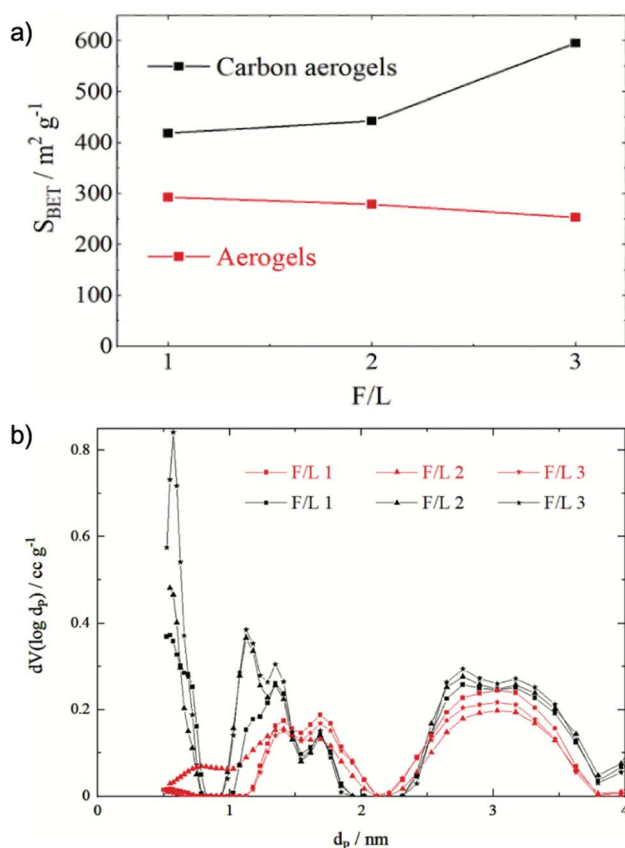

Fig. 3 (a) Correlation of initial formaldehyde–lignin mass ratio (F/L) and the specific BET surface area (S_{BET}) for resulting aerogels. (b) Pore size distributions of the aerogels (red) and carbon aerogels (black) made from solutions with different ratios of F/L[52] (Reprinted from Aufischer, G., Kamm, B. and Paulik, C., Polycondensation of kraft-lignin toward value-added biomaterials: carbon aerogels, *International Journal of Biobased Plastics*, 2021, **3**, 19–28, Creative Commons Attribution License).

2.3 Aerogels from whole biomass

Aerogels from whole lignocellulose with little or without treatment have currently attracted attention as they minimize steps and utilize all components in biomass. Aerogels from lignocellulosic biomass could be prepared *via* the dispersion route. Dewaxed rice straw was used as a precursor for aerogel synthesis using two types of cross-linkers, such as PVA and cationic starch. After the MTMS coating, aerogels exhibited high hydrophobicity with a water contact angle of 150° for PVA and 137° for cationic starch aerogel.[55] This is because cationic starch tends to attract water molecules better than PVA.[56] The aerogel prepared from the entire lignocellulose biomass had a lower oil

This journal is © The Royal Society of Chemistry 2022

J. Mater. Chem. A, 2022, **10**, 23467–23482 | **23471**

adsorption capacity (13 g g^{-1}) than aerogels from pure cellulose fibers isolated from paper waste (24.4 g g^{-1})[36] and from pineapple leaf of 37.9 g g^{-1}.[40] The lower oil adsorption of the aerogels from the whole rice straw could be attributed to a lower porosity (92–94%) for whole lignocellulose biomass,[55] compared to that (97–99%) for pure cellulose.[36,40]

The dissolution of lignocellulosic materials in ILs is considered an efficient way to prepare aerogels from the whole lignocellulose biomass. Jin and co-workers used 1-allyl-3-methylimidazolium chloride (AmimCl) to dissolve waste newspaper (composed of 50% cellulose, 17% hemicellulose, 18% lignin) to prepare aerogels.[57] The aerogel had a density of 0.029 g cm^{-3} and porosity of 96.8%. The oil adsorption capacity of aerogel was 16 g g^{-1} in the first cycle, which was lower than that of pure cellulose aerogels.[36,40] In another study,[58] using AmimCl as a dissolution solvent to prepare aerogel from *Trema orientalis* wood powder (composition unknown), it was found that aerogels had similar porosity of 97% compared to others,[57] with a density range of 0.14–0.16 g cm^{-3}.

Even though the synthesis of aerogels from the whole (untreated) lignocellulosic biomass would minimize the use of chemicals and material loss, this approach has not drawn much attention from researchers. It could be due to the lower SA of the prepared aerogels from lignocellulose compared to that of lignin-free cellulose aerogels with the current synthesis approaches. Pure cellulose aerogel had an SA of 520 m^2 g^{-1}, whereas synthetic lignocellulose aerogel and spruce wood aerogels had an SA of 213 and 122 m^2 g^{-1}, respectively.[22] In another study where aerogels with and without lignin were prepared from whole Douglas fir biomass dissolved in lithium bromide molten salt hydrate,[59] it was found that an aerogel with lignin removal step had a lower density of 0.005 g cm^{-3} and higher porosity of 99% than an aerogel with almost lignin retained (density of 0.025 g cm^{-3} and porosity of 98.3%). Similar reported results indicated that increasing lignin content (2.26% to 4.27%) increased the pore size (12 to 18 nm), therefore, decreasing the SA (146 to 51 m^2 g^{-1}).[60]

However, the applications of aerogels have mainly focused on oil adsorption, heat, and sound insulation, therefore, other properties of aerogels have not been exploited. To date, cellulose extracted from various feedstocks has been used, but the effects of the properties of the starting materials and synthetic conditions have not been fully understood. Even though previous studies have suggested that pure cellulose aerogels have better properties (*e.g.*, large SA, high porosity, low density) than aerogels prepared from lignin, hemicellulose, or a mixture of more than one component, the evidence, and understanding as to why there is such a difference is not been known or reported. Therefore, further investigation needs to be performed to provide a better understanding, such as, how cellulose interactions with one another (lignin, hemicellulose) affect the properties of aerogels.

2.4 Performance of aerogels from lignocellulose

Table 2 presents a comparison of the performance of aerogels derived from lignocellulose and aerogels from other materials.

Overall, lignocellulosic aerogels have comparable performance to other aerogels and commercially available materials. In some cases, lignocellulosic aerogels have superior performance over other types of aerogels and commercial products. For instance, for oil adsorption, banana peels and wool waste aerogels have oil adsorption of 115 and 136 g$_{oil}$ g$_{aerogel}$$^{-1}$, respectively. The adsorption capacity of those aerogels is nearly 5–9 times higher than that of the polyurethane sponge or commercial polypropylene. For sound insulation, pineapple leaf aerogels clearly have the highest sound reduction coefficient, higher than that of other types of aerogels and commercial Basmel insulation materials. On the other hand, aerogels from lignocellulose appear to have quite reasonable mechanical properties, compared to others. One aerogel having the highest compressive Young's modulus is rubber aerogels, which is understandable, due to the nature of rubber.

The survey shows that aerogels from lignocellulose have good thermal conductivity, high oil adsorption capacity as well a high noise reduction coefficient, and good mechanical properties. The properties of lignocellulosic aerogels are comparable to those of commercial materials and other types of aerogels. By using low-cost, abundant materials, aerogels from lignocellulose have become more attractive for engineering applications (thermal insulation, oil-spill removal) due to their sustainability and affordability.

2.5 Parameters affecting aerogel properties

2.5.1 Effects of precursors/starting materials. Although aerogels from cellulose, derived from lignocellulose have been studied extensively, to date there are no studies focusing on the effect of the structure and properties of precursors on aerogels. The common approach is to use "as-received" cellulose from a wide range of extraction/pre-treatment for the aerogel synthesis. "As-received" cellulose from various celluloses from a range of biomass (*e.g.*, pineapple, wastepaper, sugarcane bagasse) and different pre-treatment approaches have different properties. Therefore, it is difficult to determine what pretreatment and what structure/properties should be used and how to control the properties of aerogel for certain applications. Therefore, it is important to understand the effects of precursors (*e.g.*, size, concentration, structure, and degree of polymerization) on the resultant aerogels so that strategies for the pre-treatment and synthesis could be proposed accordingly.

Aerogels exhibit either a 3D-web-like structure or a 2D-sheet-like structure, which is found to be directly dependent on the size of the fibers. In one study, Chen *et al.* used four different nano fibrillation processes (high-intensity ultrasonication (HIUS), 20 wt% HCl hydrolysis (HCl), tetramethyl-1-piperidinyloxy (TEMPO)-mediated oxidation (TMP), and 65 wt% H$_2$SO$_4$ hydrolysis (HSO)) to treat cellulose to obtain nanocellulose fibers (NCFs)) for aerogel synthesis.[75] Thin (50–300 nm) and long fibers prepared using HIUS and TMP techniques were less intertwined. As a result, aerogels exhibited a 3D-web-like structure (Fig. 4a and e). In contrast, the NCFs obtained from HCl and HSO are larger (150–900 nm) and aggregated, creating aerogels with a 2D-sheet-like structure

23472 | *J. Mater. Chem. A*, 2022, **10**, 23467–23482

This journal is © The Royal Society of Chemistry 2022

Table 2 The performance of lignocellulosic aerogels and other materials

Materials	Oil adsorption ($g_{oil}\ g_{aerogel}^{-1}$)	Thermal insulation (mW m K^{-1})	Sound insulation (noise reduction coefficient)	Mechanical properties (kPa)	Ref.
Aerogels derived from lignocellulose					
Sugarcane aerogels	25	31–42	—	88	9
Pineapple aerogels	38	30–34	0.52	0.47–7.86	28 and 40
Spent coffee grounds aerogels	16	—	—	15.6	41
Banana peels	115	—	—	—	61
Wool waste	136	—	—	26.7–53.48	62
Aerogels from other materials					
Rubber aerogels	25	35–49	0.41–0.56	3.85–965	63–65
rPET aerogels	79	35–38	0.45	1.16–2.87	66 and 67
Magnesium hydroxide aerogels	—	30–42	0.44–0.49	7.9–49.3	68
Red mud aerogels	30	18–22	—	—	47
Dislodged sludge aerogels	—	30–32	—	—	69
Coal gangue aerogels	—	20–32	—	—	70
Commercial products & others					
Carbon nanotubes	17	—	—	—	71
Polyurethane sponge	23	—	—	—	72
Commercial polypropylene	15	—	—	—	62
Graphene oxide	80	—	—	—	73
Polyurethane foam	—	24	—	—	74
Polystyrene foam	—	41	—	—	74
Mineral wool	—	35–44	—	—	74
Commercial basmel	—	—	0.4	—	66

(Fig. 4c and f).[75] Nevertheless, at higher concentrations of NCFs (e.g., 0.5 wt%), the NCFs are larger and eventually aggregated into a 2D-sheet-like structured aerogel after freezing regardless of nano-fibrillation method (Fig. 4a, b, d, f, and h). Similar findings were also reported,[76] in that, NCFs prepared using 64 wt% H_2SO_4 were aggregated, forming 2D-sheet-like structured aerogels.

In conclusion, thin fibers are less self-aggregated, producing 3D-web-like structured aerogels, whereas large fibers tend to self-aggregate, leading to 2D-sheet-like structured aerogels. The structure of aerogels does have an impact on the properties of aerogels. In one study,[77] cellulose fractionated from sugarcane bagasse was used to prepare aerogels for drug delivery carriers. At low concentrations (1% w/v), fibers were thin and had less aggregation, forming a 3D-web-like structured aerogel with a large SA (525 m^2 g^{-1}). When the concentration of cellulose increased to 5% w/v, fibers aggregated, leading to a 2D-sheet-like structured aerogel with a lower SA (22 m^2 g^{-1}).

The molecular weight of the precursors also affects the properties of aerogels. However, the effects are inconsistent. For example, at the same experimental conditions, the surface area of an aerogel prepared with cellulose (M_w = 86 000 g mol^{-1}) is 20% lower than that of the one prepared with lower molecular weight cellulose (M_w = 52 000 g mol^{-1}).[44] In contrast, Rosta-mitabar et al. reported the opposite effect of molecular weight of cellulose on SA of aerogels[46] using two types of microcrystalline cellulose powders, C6288 (M_w = 163 500 g mol^{-1}) and S6790 (M_w = 565 630 g mol^{-1}). The two types of cellulose were dissolved using calcium thiocyanate tetrahydrate (Ca(SCN)$_2$·4H$_2$O) salt and regenerated before being dried to obtain aerogels.[46] It was reported that the aerogel prepared with high molecular weight cellulose (C6288) had a higher surface area, denser structure, and better thermal stability than the aerogel obtained from low molecular weight cellulose (S6790). This was explained due to the effect of the structure of fibers as C6288 cellulose had thinner fibers and smaller crystallinity,[46] which are less likely to self-aggregate[78] as the higher the aggregation, the lower the pore volume and SA. The discrepancy in the effect of molecular weight on aerogels' properties has not been fully understood, therefore interactions between properties of precursors (DP, size of fibers, impurities etc.) and operating conditions need to be studied further.

Increasing the concentration of precursors increases the density, making the aerogel less porous,[79] as shown in Fig. 5a–c therefore, increasing thermal conductivity[9] and the noise reduction coefficient.[28] Furthermore, increasing cellulose concentration results in a denser structure with a 2D-sheet-like morphology, because the fiber–fiber interaction surpasses the water–fiber interaction.[79] Moreover, a high cellulose concentration promotes the aggregation of cellulose nanofibers, therefore, lowering the SA (Fig. 5d).[80]

2.5.2 Effects of drying methods. Drying, which is to replace the liquid in the pores of the aerogel with air is currently considered the most important step in the preparation of aerogels. In ambient drying, the liquid in the wet gel is evaporated (from the liquid phase (L) to the gas phase (G), crossing the liquid–gas (L–G) equilibrium curve, Fig. 6). Thus, the gas–liquid menisci appear at the pore boundaries, creating the induced capillary stresses, which might cause the gel structure to collapse. Therefore, in the preparation of aerogels, drying must

This journal is © The Royal Society of Chemistry 2022

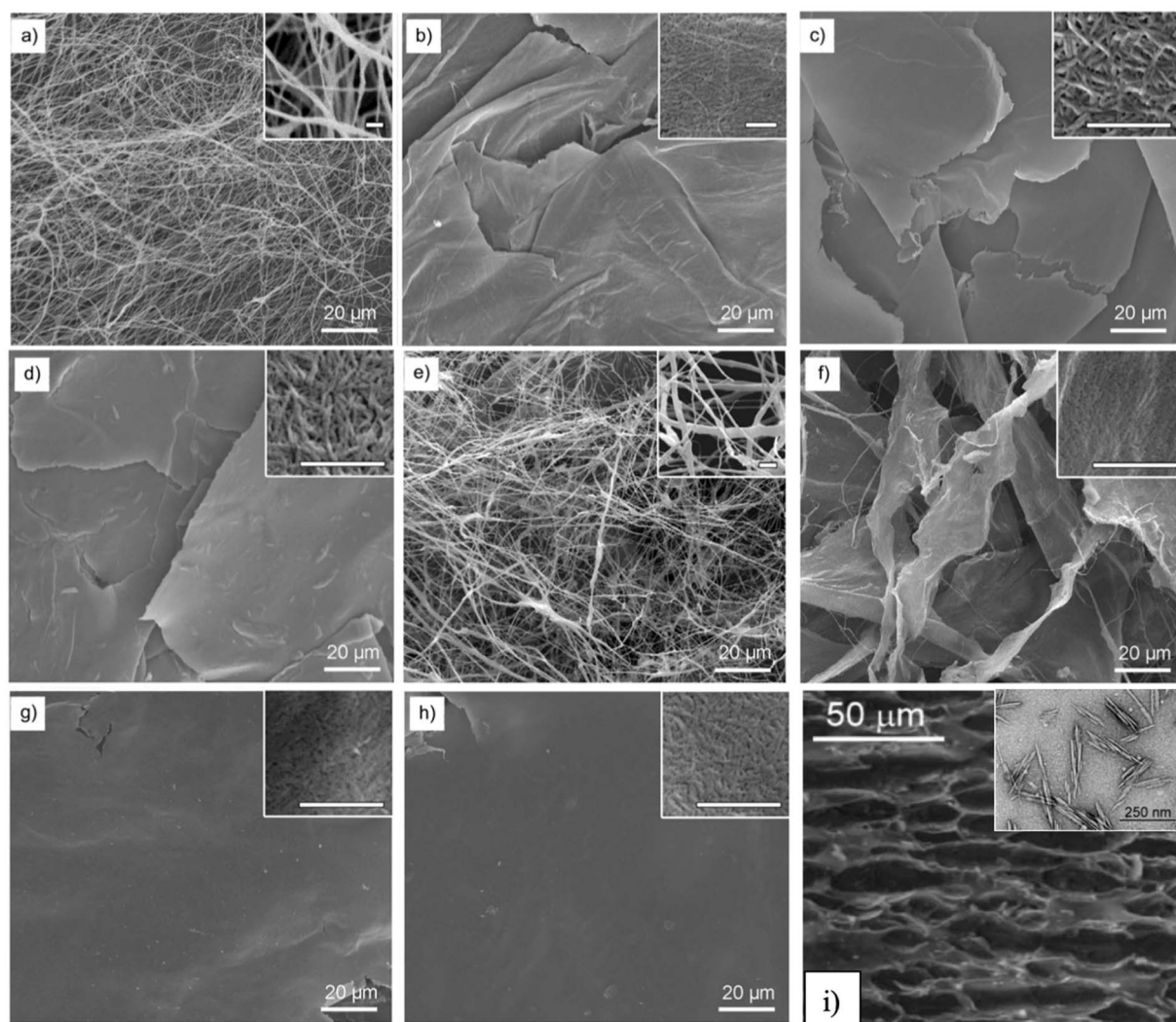J. Mater. Chem. A, 2022, **10**, 23467–23482 | **23473**

Fig. 4 SEM images of NCF aerogels: (a, b) HIUS-NCF aerogel, (c, d) HCl-NCF aerogel, (e, f) TMP-NCF aerogel, and (g, h) HSO-NCF aerogel. NCF contents: (a, c, e, g) 0.1 wt% and (b, d, f, h) 0.5 wt%. The scale bars in the insets of all images correspond to 1 mm (Reprinted with permission from Chen, W., Li, Q., Wang, Y., Yi, X., Zeng, J., Yu, H., Liu, Y. and Li, J., Comparative Study of Aerogels Obtained from Differently Prepared Nano-cellulose Fibers, *ChemSusChem*, 2017, **7**, 54–161),[75] (i) cellulose nanowhisker aerogel, the inset is the TEM image of cellulose nanowhiskers (Reproduced from ref. [76] with permission from the Royal Society of Chemistry). Acronyms: HIUS: high-intensity ultrasonication, HCl: 20 wt% HCl hydrolysis, TMP: tetramethyl-1-piperidinyloxy (TEMPO)-mediated oxidation (TMP), HSO: 65 wt% H_2SO_4 hydrolysis.

annihilate the liquid surface tension, in other words, avoid crossing the liquid–gas equilibrium curve.[17]

There are two common choices for drying aerogels that eliminate capillary stresses: supercritical drying and freeze-drying. In supercritical drying, temperature and pressure are increased beyond the critical point of the liquid phase in the wet gel, which leads to the transition from the liquid phase (L) to a supercritical fluid. Then, pressure is reduced while the temperature is still maintained constant, and supercritical fluid transforms into a gas without crossing the L–G,[18] equilibrium curve (Fig. 6). In freeze-drying, liquid in the wet gel is first frozen (to a solid phase (S)) and thereafter sublimated (Fig. 6). Again,[14,18] the L–G equilibrium curve is not crossed, thus, liquid–gas menisci are prevented.

In terms of definitions, the resulting gels after drying are normally defined as aerogels (*via* supercritical drying), cryogels (*via* freeze-drying), and xerogels (*via* evaporative drying).

Comparative studies on the effects of drying techniques on the morphology of cellulose aerogels were conducted by Buchtová and Budtova[81] and Ganesan *et al.*[82] Freeze-drying and vacuum drying at atmospheric pressure led to a 2D-sheet-like structure, especially the vacuum drying, producing flat non-porous aerogels (Fig. 7). On the other hand, aerogels obtained from supercritical CO_2 drying might have a cauliflower-like structure[81] or a honeycomb-like structure.[82]

The volume shrinkage of aerogels *via* vacuum drying is 87–97% compared to 21–66% *via* supercritical drying, and 7–22% *via* freeze-drying. Ganesan *et al.* (2016) reported that ambient drying had a volume shrinkage of 90 compared to 16% and 40%

23474 | *J. Mater. Chem. A*, 2022, **10**, 23467–23482

This journal is © The Royal Society of Chemistry 2022

Fig. 5 X-ray microtomography analysis of nano-fibrillated cellulose aerogels (a) 3D image of 0.75 wt% aerogel, (a′ and a″) top and bottom side slice (2D) images of 0.75 wt% aerogel; (b) 3D image of 1.00 wt% aerogel, (b′ and b″) top and bottom side slice (2D) images of 1.00 wt% aerogel; (c) 3D image of 1.75 wt% aerogel, (c′ and c″) top and bottom side slice (2D) images of 1.75 wt% aerogel[79] (Reprinted from Gupta, P., Singh, B., Agrawal, A. K. and Maji, P. K., Low density and high strength nanofibrillated cellulose aerogel for thermal insulation application, *Materials & Design*, 2018, **158**, 224–236, copyright 2018, with permission from Elsevier), (d) correlation of density and BET specific surface area of the micro-fibrillated cellulose aerogels (Reproduced from ref. [80] with permission from the Royal Society of Chemistry).
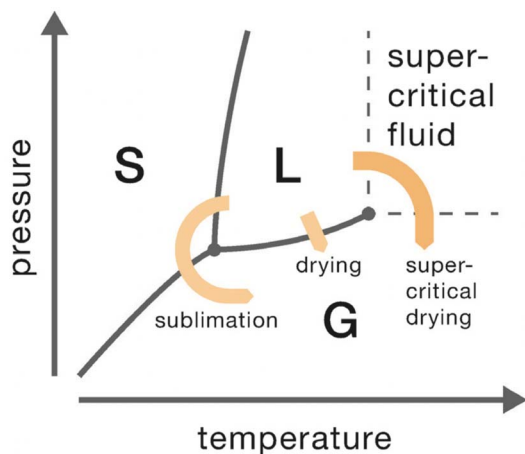

Fig. 6 Phase diagram of the liquid to be removed from the gel network. Reprinted with permission from Ziegler, C., Wolf, A., Liu, W., Herrmann, A.-K., Gaponik, N. and Eychmüller, A., Modern Inorganic Aerogels, *Angewandte Chemie International Edition*, 2017, **56**, 13200–13221.

for supercritical drying and freeze-drying, respectively.[82] It is because vacuum drying is slow and induces strong capillary pressures on the pore walls.[81] However, the volume shrinkage is reported to be cellulose concentration-dependent, *e.g.*, the higher the cellulose concentration, the lower the volume shrinkage because more cellulose creates strong pore walls, which in turn resist the capillary stress.[81] The porosity of aerogels from supercritical drying and freeze-drying is high (86–97%) compared to 2–5% from vacuum drying.[81,82] It is because supercritical and freeze-drying did not cause the collapse of large pores and channels during drying, while high capillary stress caused by evaporative drying leads to the collapse of the pores.

Supercritical drying produces aerogels with the highest SA (239–312 m^2 g^{-1}) due to their multiscale nanostructure.[81,82] On the other hand, freeze-drying causes the growth of ice crystals, which forces cellulose nanofibrils to the crystal boundaries aggregate during the freezing process, thus resulting in the thin sheet form aerogels and larger macropores.[42] Due to the larger pores of aerogels, SA (10–60 m^2 g^{-1}) is much smaller than those of aerogels from supercritical drying. Similar results were reported for aerogels with large macropores that had SA in the same range of 10–60 m^2 g^{-1}.[80,82,83] The SA of aerogels obtained from vacuum drying was reported to be about 1 m^2 g^{-1}.[81]

This journal is © The Royal Society of Chemistry 2022

J. Mater. Chem. A, 2022, **10**, 23467–23482 | **23475**

Fig. 7 SEM of cellulose aerogels obtained from (a) supercritical CO_2 drying, (b) freeze–drying, (c) evaporative drying, the insets are aerogel samples.[82] Reprinted from Ganesan, K., Dennstedt, A., Barowski, A. and Ratke, L., Design of aerogels, cryogels and xerogels of cellulose with hierarchical porous structures, *Materials & Design*, 2016, **92**, 345–355, copyright 2016, with permission from Elsevier.

In two studies, the effects of drying techniques on aerogels[81,82] were studied, an interesting finding was that xerogels (from evaporative drying)[81] badly shrunk with the structure almost collapsing (porosity less than 5%), whereas xerogels produced by Ganesan *et al.* were still porous 70–80%, even though the volume shrinkage was nearly the same (89–93%). The difference could be due to the surface tension of the solvents used in the coagulation and washing steps. The greater surface tension of water (0.073 N m^{-1} at 20 °C) caused the severe volume shrinkage, leading to a strong agglomeration of nanofibrils, consequently an extremely poor porous network compared to isopropanol and ethanol surface (surface tension of 0.0233 and 0.0224 N m^{-1}). During the evaporative drying, the vapor pressure of the solvent was also found to affect the morphology of the resulting xerogels. For instance, the faster evaporation rate of ethanol due to high vapor pressure leads to a higher volume shrinkage and densification, which in turn makes the agglomerated fibers less porous and of low SA. More specifically, xerogel with isopropanol filled in pores had a porosity of 80% and SA of 107 m^2 g^{-1}, while xerogel with ethanol was less porous (70%) and had extremely low SA (0.87 m^2 g^{-1}).[82]

2.5.3   Types of cross-linking agents. Several types of cross-linkers (PVA,[28] Kymene,[29] and cationic starch[55]) have been investigated in the preparation of aerogels from lignocellulosic components. However, it is worth mentioning that the use of cross-linkers is needed only if aerogels are prepared *via* a dispersion route. Based on the literature survey, the number of comparative studies of different cross-linking agents on the performance or properties of aerogels is very limited. In one study, cellulose aerogels were prepared with four different cross-linkers with cellulose to synthesize aerogels, including polyester resin, cellulose acetate, starch, and a mixture of starch and cellulose acetate.[84] The results show that the density of aerogel samples with different cross-linkers is in the order of polyester resin > starch > start-cellulose acetate > cellulose acetate. The compression modulus can be linearly proportional to the density. Because porosity decreases with increasing density, the compression moduli are inversely proportional to the porosity. Oil adsorption of aerogels is a physical phenomenon depending on the porosity, the oil adsorption capacity thus increases with the increase of porosity.[84] In another study, Loh *et al.* investigated the effects of cross-linker (PVA) concentration on the properties of aerogels from waste wool.[62] The results show that increasing either PVA or cellulose will increase the density of aerogels, effectively decreasing the porosity, which in turn reduces the oil adsorption capacity. So far, the explanation regarding the effect of cross-linkers on aerogels' properties is heavily correlated with density and porosity.

Even though different cross-linkers have been used, the choice is rather arbitrary, and the mechanism of cross-linking and its effects have not been well understood.

2.6   Materials and synthesis routes

Currently, there is no standard as to which materials should be used and what synthesis should be chosen to prepare lignocellulose aerogels. It could be because the synthesis of aerogels from lignocellulose is still in its exploring phase. Aerogels from cellulose could be used for certain applications, such as water treatment, catalyst, drug delivery, heat, and sound insulation, from which the corresponding starting material and synthesis route could be chosen accordingly.

Based on the survey, the fabrication strategies for certain applications are suggested, as shown in Fig. 8. The water treatment application of aerogels is *via* adsorption, thus, the large SA, high porosity, and abundant reactive functional groups are desirable. For instance, the dispersion[9] and dissolution[36] routes offer the same oil adsorption capacity of 25 (g per oil) (g per aerogel), however, high durability is desired for reusability purposes. Therefore, the dispersion is chosen over the dissolution route. Also, oil adsorption is a physical phenomenon occurring *via* pore-filling, thus, high porosity is expected, and cellulose is chosen as a preferred material. The aerogel prepared from the entire lignocellulose biomass has a lower oil adsorption capacity (13 g g^{-1})[55] than those from the lignin-free cellulose fibers fractionated from paper waste (24.4 g g^{-1})[36] and pineapple leaf (around 38 g g^{-1}).[40] The carbonization step could significantly increase the adsorption capacity of aerogels up to 106–312 g g^{-1}.[85] Under the same synthetic conditions, cellulose aerogels exhibit better properties (large SSA and higher porosity) than those derived from lignin or hemicellulose (as mentioned in Section 2.4). Therefore, in applications (*e.g.*, dye removal), where SA is crucial, lignin-free cellulose is preferred as the starting material to prepare aerogels. Huang *et al.* reported that cellulose-derived carbon aerogels with SA (2825 m^2 g^{-1}) had a methylene blue adsorption capacity (1078 mg g^{-1}), which is nearly 5-fold higher than that of the aerogel with SA (791.4 m^2 g^{-1}).[86]

23476 | *J. Mater. Chem. A*, 2022, **10**, 23467–23482
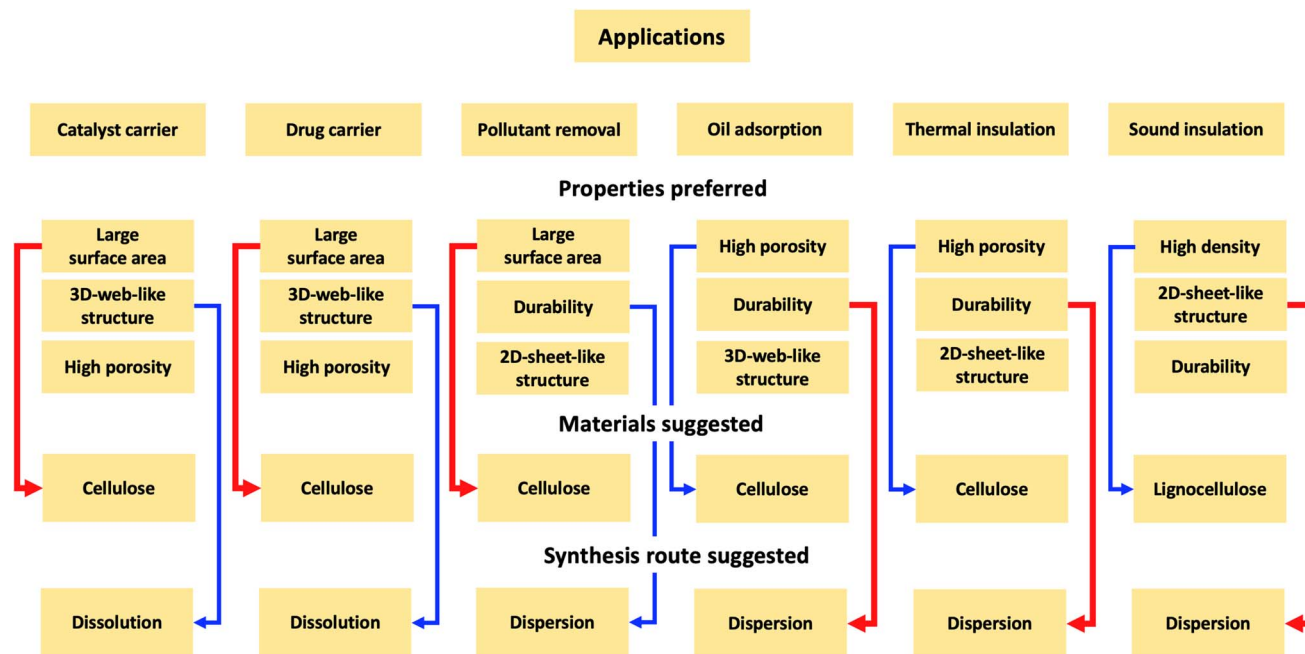
This journal is © The Royal Society of Chemistry 2022

Fig. 8 Fabrication strategies for certain applications. Properties preferred are listed in the order of priority. Materials and synthesis routes are derived from the required properties. Red arrows mean primary conditions, while blue arrows mean secondary conditions. The primary condition is chosen to achieve the most important property.

For applications such as heat and sound insulation, the aerogel performance depends on the porosity of aerogels. Due to high porosity, aerogels capture a large volume of air (air is a good insulator at ambient temperature and pressure, 0.026 W m^{-1} K^{-1}). Therefore, the higher the porosity, the lower the thermal conductivity. The dissolution route helps achieve the 3D-web-like structure for aerogels[22] with large pores and high porosity. Also, the material concentration should be kept low, because increasing the material concentration would increase the aggregation of fibers, thus decreasing the porosity.[9] The effect is, however, the opposite for sound insulation applications. Smaller pore size and less porosity would prevent sound from transmitting through the aerogel, consequently, the noise reduction coefficient increases.[28] The dispersion route and increasing material concentration would produce aerogels with a 2D-sheet-like structure with a small pore size and less porosity, therefore, increasing the noise reduction coefficient.

Aerogels have also been used as carriers such as drug delivery.[87] Aerogels must not only have high porosity and large SA for the impregnation of active compounds but also be non-cytotoxic materials. Ideally, biocompatible and biodegradable cellulose is the best choice as a precursor. However, cellulose must be lignin-free because lignin is reportedly slightly cytotoxic for peripheral blood mononuclear cells due to its phenolic nature.[88] The dissolution route offers aerogels with large SA (dispersion: 25 m^2 g^{-1}, dissolution: up to 300 m^2 g^{-1}, as shown in Table 1 above). Even though dissolution solvents like ILs have produced some controversy due to their toxicity and biodegradability, non-toxic and biodegradable cations and anions could be used to prepare low-toxicity ILs. Agostinho *et al.* prepared κ-carrageenan aerogels from two different types of ILs:

1-butyl-3-methyl imidazolium chloride (BmimCl) and 1-butyl-3-methyl imidazolium acetate (BmimAc). Both aerogels had SA ranging from 185–215 m^2 g^{-1} and a total pore volume of 0.32–0.46 cm^3 g^{-1}. More importantly, the resulting aerogels did not show cytotoxicity during the cytotoxicity test assays (Caco-2 cell for 24 hours), which are suitable for pharmaceutical applications. The aerogel prepared by the dissolution in IL having a 3D-web-like structure (Fig. 9a) has a higher loading rate of tetracycline (21.2%) and a higher release rate (0.031 mg min^{-1}) than the aerogel dissolved in water and potassium salt (loading rate: 8.8%, release rate: 0.011 mg min^{-1}), which has a 2D-sheet-like structure (Fig. 9b).[87] The higher loading rate and release rate of the aerogel prepared by IL is attributed to its higher macroporosity. The same observation was reported elsewhere.[77] The 3D-web-like structured aerogel (Fig. 9c) with the largest SA of 525 m^2 g^{-1} offered the highest loading rate of 6.4 mg g^{-1} for methylene blue and the fastest release rate (4.34% per hour), compared to the 2D-sheet-like structured aerogel (Fig. 9d) with SA of 22 m^2 g^{-1}, whose loading rate was 0.8 mg g^{-1} and release rate was 2.5% per hour.[77] The same properties (larger SA and high porosity) are recommended for aerogels to be used as catalyst supports. Normally, the carbonization of aerogels into carbon aerogels is recommended to offer even larger SA (400–1000 m^2 g^{-1}) and durability.[89,90]

3 Challenges and future development of the lignocellulosic aerogel

Aerogels from lignocellulose have been studied, but the effects of synthetic conditions and the nature of starting materials on
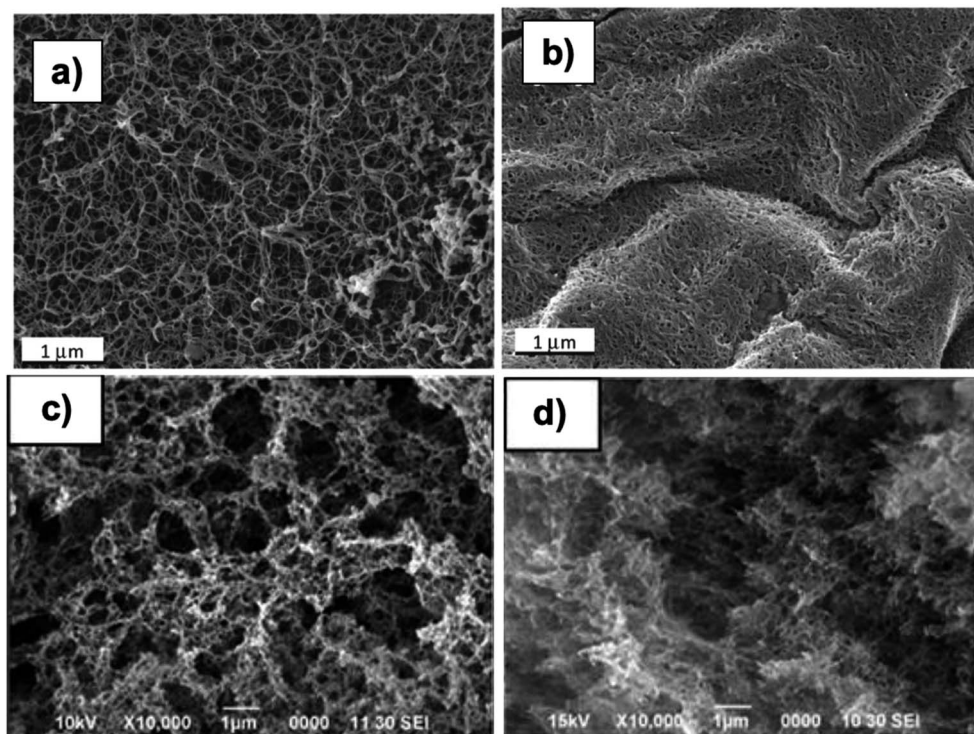
This journal is © The Royal Society of Chemistry 2022

J. Mater. Chem. A, 2022, **10**, 23467–23482 | **23477**

Fig. 9 SEM images of κ-carrageenan aerogel samples: (a) dissolved in BmimCl, (b) dissolved in water and KCl[87] (Reprinted from Agostinho, D. A. S., Paninho, A. I., Cordeiro, T., Nunes, A. V. M., Fonseca, I. M., Pereira, C., Matias, A. and Ventura, M. G., Properties of κ-carrageenan aerogels prepared using different dissolution media and its application as drug delivery systems, *Materials Chemistry and Physics*, 2020, **253**, 123290, copyright 2020, with permission from Elsevier). SEM images of sugarcane bagasse aerogel samples prepared by dissolution in NaOH : thiourea : urea (8 : 6.5 : 8 w/v%): (c) 1 wt%, (d) 5 wt% (Reprinted with permission from Chin, S.-F., Jimmy, F. B. and Pang, S.-C., Fabrication of Cellulose Aerogel from Sugarcane Bagasse as Drug Delivery Carriers, *Journal of Physical Science*, 2016, **27**, 159–168).[77]

the properties of aerogels have not been investigated. For instance, in the dispersion route when pure cellulose is used, the effects of cross-linkers (type, concentration), the reaction time of the cross-linking reaction, dispersion time, or the power of ultrasonic have not been investigated. For the dissolution route, the regeneration of cellulose has been studied, however,
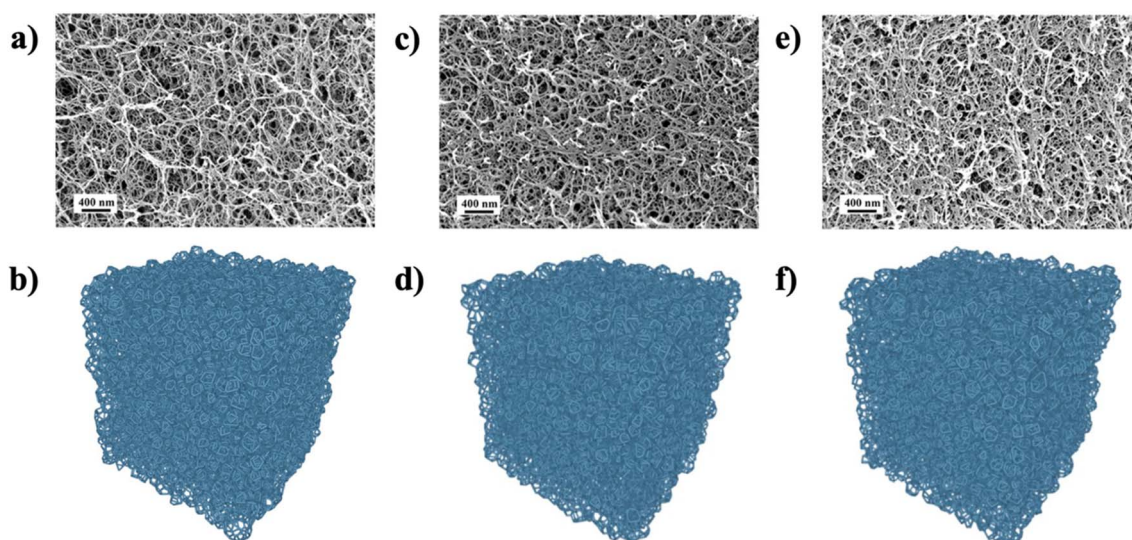

Fig. 10 SEM images of κ-carrageenan aerogels (top row) and the computationally designed nanostructured aerogel network (bottom row) of 1 wt% (a, b), 2 wt% (c, d) 3 wt% (e, f) κ-carrageenan[96] (Adapted from Chandrasekaran, R., Hillgärtner, M., Ganesan, K., Milow, B., Itskov, M. and Rege, A., Computational design of biopolymer aerogels and predictive modelling of their nanostructure and mechanical behaviour, *Scientific Reports*, 2021, **11**, 10198, Creative Commons Attribution 4.0 International License).

the changes in cellulose fibers before and after regeneration and drying on the properties of aerogels have not been investigated. It is unclear whether the structure of aerogels could be replicated under the same conditions. Different lignocellulose resources and pre-treatment methods have been used to obtain cellulose fibers, but the effects of the composition of fibers (cellulose, hemicellulose, and lignin contents) on aerogels' properties have not been well understood. Furthermore, there is a lack of evidence for the mechanisms of how changes in certain parameters would result in the differences in aerogels' properties. Understanding the mechanisms of aerogel formation and its properties is important for process development.

Most studies have focused on pure components, such as cellulose isolated from lignocellulose biomass as evidenced that aerogels from pure cellulose tend to have better properties, such as high SA and porosity. Nonetheless, the use of pure cellulose could increase the production cost, hence hindering its commercialization. An alternative way to produce aerogels without any pre-treatment is via direct dissolution of lignocellulose in ILs, which minimizes the amount of waste stream and material lost. However, it is worth mentioning that some ILs are toxic[91] and expensive, ranging from 400 to 20 000 EUR per kg,[92] and the process still involves the separation of ILs from antisolvent and water during coagulation and washing steps. The capital costs could reduce significantly if ILs could be fully recovered, for instance, via nanofiltration membrane[93] or pervaporation.[94] Furthermore, direct dissolution utilizes all three major components of lignocellulose: cellulose, hemicellulose, and lignin. Even though it has been reported that coupling cellulose, hemicellulose, and lignocellulose results in aerogels with poorer properties in comparison to pure cellulose aerogels (as mentioned in Section 2.4), the intensification of the synthesis route could be performed to overcome the limitations of aerogels from the whole lignocellulose. For instance, the homogenization of the mixture after the dissolution proved to reduce the particle size, thus enhancing the cellulose solubilization and lignin dispersion, hence improving the homogeneity and properties of the aerogel. As a result, an aerogel prepared with a homogenization step has a larger surface area (105 m^2 g^{-1}) than that without the homogenization (60 m^2 g^{-1}).[59] Carbonization can be used to further improve the properties of aerogels prepared from the entire lignocellulose biomass. For instance, the normal aerogels without the carbonization step had pore volume in the range of 0.1×10^{-3} to 3.5×10^{-3} cm^3 g^{-1}, SA in a range of 2.5–34 m^2 g^{-1}. The properties such as pore volume and SA could be enhanced more than 100 times after carbonization, for instance, a carbon aerogel could possess pore volume and SA of up to 2 cm^3 g^{-1} and 2825 m^2 g^{-1}, respectively.[86]

Precursors such as cellulose, lignin, and hemicellulose have been used to prepare aerogels. The differences in aerogels' properties (porosity, surface area, mechanical strength) have been reported, but the reasons why there is such a difference have not been fully understood. Therefore, it is important to have a fundamental understanding in terms of material sciences, such as how changes in certain components affect the structure of aerogels, and thus the aerogel properties. In this

regard, molecular modeling is useful for answering questions related to aerogel structures, preparation, and properties. There are two main approaches in simulations of aerogels, including atomistic descriptions and coarse-grained descriptions. The former treats each atom individually, while the latter treats larger objects assembled by many atoms of molecules.[95] Both approaches have been used extensively on silica aerogels, which are synthesized via the sol–gel process from monomers while starting materials of aerogels from lignocellulosic components are 'already' polymers. Therefore, the aforementioned approaches might not be applicable to the aerogels derived from lignocellulose.

An alternative to modelling porous materials like biopolymer aerogels, including but not limited to cellulose aerogels, is reconstruction, where experimental data are inverted to generate a computational realization of the material structure. In a recent study, Chandrasekaran et al. developed a computational approach, using the Laguerre–Voronoi tessellation (LVT) based on random closed packing of polydisperse spheres (RCPPS). It was reported that the nanostructure and mechanical behavior of κ-carrageenan aerogels could be predicted if the pore size distributions (PSD), solid fractions, and Young's modulus of the pore-wall fibers are known.[96] Fig. 10 presents SEM images and computational designs of the nanostructure of κ-carrageenan aerogels at different concentrations. The computational designs represent quite well the actual fibrillar morphology of the aerogels. The higher the κ-carrageenan content, the denser the aerogel and the smaller the pores. Furthermore, the simulation results of pore size distribution and mechanical behaviors are in good agreement with experimental ones.[96] There have been several attempts to close the gap between theory and experiments and further understand the structure–property relationship of biopolymer aerogels, such as a generalized micro-mechanical model[97] or bonded-particle model coupled with discrete element method[98] to model mechanical behaviors of biopolymer aerogels. Nonetheless, the findings of Chandrasekaran and colleagues are sui generis, which, based on attainable data (e.g., PSD, solid fractions, and Young's modulus), showed that a 3D computationally designed structure of aerogels is feasible to tailor properties and applications accordingly.

4 Conclusions

This work reviewed the current development in the preparation of aerogels from cellulose, hemicellulose, and lignin-derived from lignocellulose biomass. The dispersion route produces aerogels with a 2D-sheet-like structure, whereas the dissolution route leads to a 3D-web-like structure aerogel. 3D-web-like structured aerogels possess a high SA and porosity. However, when the concentration of precursor increases, the self-aggregation increases, and aerogels would only exhibit a 2D-sheet-like structure regardless of the synthetic route. The structural properties of fibers have a strong effect on the structure of aerogels, e.g., if fibers are well separated by nanofibrillation methods, aerogels would have a 3D-web-like structure, whereas aerogels would end up having a 2D-sheet-like

This journal is © The Royal Society of Chemistry 2022

J. Mater. Chem. A, 2022, 10, 23467–23482 | 23479

structure if fibers are already aggregated before the synthetic step.

Evaporation drying seems unsuitable with the current development. Supercritical drying produces aerogels with minimum destruction, followed by freeze-drying. However, the suggested drying method was only for retaining the structure of aerogels at the drying stage and neglecting the effects of synthetic conditions. There are no available studies on the interactions between the synthetic and drying steps on the structure of aerogels. Therefore, it can be hypothesized that the evaporative drying could still be as effective either if the solvent used during the synthetic approach has a low surface tension and evaporation rate to reduce the volume shrinkage and agglomeration or if the materials from the gel process are sufficient to resist the collapse of the structure. Drying cannot be a "stand-alone" step but must be studied in conjunction with others to aid the development of aerogel production from lignocellulosic materials.

Chemical pre-treatment approaches are used to obtain cellulose for aerogels and they ignore other components, leading not only to up to 50% loss of materials (lignin and hemicellulose) but also posing an environmental threat due to the use of harsh chemicals. An alternative way is to fractionate the lignocellulosic biomass or dissolve the entire lignocellulosic biomass in dissolution solvents, such as ILs for preparing aerogels. This will not only reduce the capital costs but also minimize materials lost. However, two aspects need to be further studied: (1) the recoverability of ILs that would help reduce the costs and waste stream, (2) the intensification of pre-treatment and synthetic aerogels.

Studies of aerogels from lignocellulose are still focusing on exploring new lignocellulose sources and the choice of synthesis routes. The mechanism of cellulose, hemicellulose, and lignin interaction after dissolution, regeneration, and drying, and how the interaction affects the properties of aerogels are not fully understood. The effects of the molecular size of polymers, and synthesis conditions on their properties have not been fully investigated. Certain things could be considered to provide further understanding: (1) more advanced characterization techniques such as nano-CT as a super high-resolution imaging technique to study the change in textural properties of fibers, (2) mathematical modeling of gel formation and nanostructure of aerogel accordingly that would help predict the structural properties and produce aerogels in a customizable manner.

To date, aerogels from lignocellulose are still in their infancy and previous studies have focused on exploring starting materials, and synthesis routes rather than discussing the mechanisms behind the changes in aerogels' structures and properties caused by synthetic conditions. There is an urgent need to better understand such changes as it will help engineers to design aerogels with desired properties. Production of aerogels derived from lignocellulose is still emerging, but a sustainable way to turn biomass into value-added products. Still, several aspects need a better understanding, and this review is expected to stimulate further research in this direction.

Conflicts of interest

There are no conflicts to declare.

Acknowledgements

References

1 L.-Y. Long, Y.-X. Weng and Y.-Z. Wang, *Polymers*, 2018, **10**, 623.

2 P. T. T. Nguyen, N. H. N. Do, X. Y. Goh, C. J. Goh, R. H. Ong, P. K. Le, N. Phan-Thien and H. M. Duong, *Waste Biomass Valorization*, 2022, **13**, 1825–1847.

3 E. Cuce, P. M. Cuce, C. J. Wood and S. B. Riffat, *Renew. Sustain. Energy Rev.*, 2014, **34**, 273–299.

4 L. Wen Zhen, Q. B. Thai, T. X. Nguyen, D. K. Le, J. Kai Wei Lee, Y. Qing Xiang and H. M. Duong, *Fluids*, 2019, **4**, 174.

5 N. H. N. Do, V. T. Tran, Q. B. M. Tran, K. A. Le, Q. B. Thai, P. T. T. Nguyen, H. M. Duong and P. K. Le, *J. Polym. Environ.*, 2021, **29**, 1112–1121.

6 H. Maleki and N. Hüsing, *Appl. Catal. B Environ.*, 2018, **221**, 530–555.

7 L. M. Sanz-Moral, A. Aho, N. Kumar, K. Eränen, M. Peurla, J. Peltonen, D. Y. Murzin and T. Salmi, *Catal. Letters*, 2018, **148**, 3514–3523.

8 K. Gu, E. J. Kim, S. K. Sharma, P. R. Sharma, S. Bliznakov, B. S. Hsiao and M. H. Rafailovich, *Mater. Today Energy*, 2021, **19**, 100560.

9 Q. B. Thai, S. T. Nguyen, D. K. Ho, T. Du Tran, D. M. Huynh, N. H. N. Do, T. P. Luu, P. K. Le, D. K. Le, N. Phan-Thien and H. M. Duong, *Carbohydr. Polym.*, 2020, **228**, 115365.

10 H. Li, Z. Wang, X. Liu, F. Cui, C. Chen, Z. Zhang, J. Li, L. Song and R. Bai, *Chem. Phys. Lett.*, 2020, **755**, 137805.

11 Y. Yu, X. Shi, L. Liu and J. Yao, *J. Mater. Sci.*, 2021, **56**, 2763–2776.

12 N. Hüsing and U. Schubert, *Angew. Chem., Int. Ed.*, 1998, **37**, 22–45.

13 J. Stergar and U. Maver, *J. Sol-Gel Sci. Technol.*, 2016, **77**, 738–752.

14 A. C. Pierre and G. M. Pajonk, *Chem. Rev.*, 2002, **102**, 4243–4266.

15 M. H. Mruthunjayappa, D. Mondal and S. K. Nataraj, in *Polymer Aerogels for Energy Storage and Water Purification Applications*, 2022, pp. 31–52, DOI: **10.1007/978-981-16-8755-6_3**.

16 D. K. Sam, E. K. Sam, A. Durairaj, X. Lv, Z. Zhou and J. Liu, *Carbohydr. Res.*, 2020, **491**, 107986.

17 A. C. Pierre and A. Rigacci, in *Aerogels Handbook*, Springer New York, New York, NY, 2011, pp. 21–45.

18 C. Ziegler, A. Wolf, W. Liu, A.-K. Herrmann, N. Gaponik and A. Eychmüller, *Angew. Chem., Int. Ed.*, 2017, **56**, 13200–13221.

23480 | *J. Mater. Chem. A*, 2022, **10**, 23467–23482

This journal is © The Royal Society of Chemistry 2022

19 L. Hu, R. He, H. Lei and D. Fang, *Int. J. Thermophys.*, 2019, **40**, 39.

20 K. Ganesan, T. Budtova, L. Ratke, P. Gurikov, V. Baudron, I. Preibisch, P. Niemeyer, I. Smirnova and B. Milow, *Materials*, 2018, **11**, 2144.

21 Y. Fang, S. Chen, X. Luo, C. Wang, R. Yang, Q. Zhang, C. Huang and T. Shao, *RSC Adv.*, 2016, **6**, 54054–54059.

22 O. Aaltonen and O. Jauhiainen, *Carbohydr. Polym.*, 2009, **75**, 125–129.

23 M. A. Karaaslan, J. F. Kadla and F. K. Ko, in *Lignin in Polymer Composites*, Elsevier, 2016, pp. 67–93.

24 T. Budtova, *Cellulose*, 2019, **26**, 81–121.

25 A. Zaman, F. Huang, M. Jiang, W. Wei and Z. Zhou, *Energy Built Environ.*, 2020, **1**, 60–76.

26 H. M. Duong, N. R. B. Ling, Q. B. Thai, D. K. Le, P. T. T. Nguyen, X. Y. Goh and N. Phan-Thien, *Waste Manag.*, 2021, **124**, 1–7.

27 H. Zhang, Y. Li, Y. Xu, Z. Lu, L. Chen, L. Huang and M. Fan, *Phys. Chem. Chem. Phys.*, 2016, **18**, 28297–28306.

28 N. H. N. Do, T. P. Luu, Q. B. Thai, D. K. Le, N. D. Q. Chau, S. T. Nguyen, P. K. Le, N. Phan-Thien and H. M. Duong, *Mater. Chem. Phys.*, 2020, **242**, 122267.

29 J. Feng, S. T. Nguyen, Z. Fan and H. M. Duong, *Chem. Eng. J.*, 2015, **270**, 168–175.

30 Z. E. Lim, Q. B. Thai, D. K. Le, T. P. Luu, P. T. T. Nguyen, N. H. N. Do, P. K. Le, N. Phan-Thien, X. Y. Goh and H. M. Duong, *J. Environ. Chem. Eng.*, 2020, **8**, 104524.

31 S. T. Nguyen, J. Feng, S. K. Ng, J. P. W. Wong, V. B. C. Tan and H. M. Duong, *Colloids Surf., A*, 2014, **445**, 128–134.

32 M. Deng, Q. Zhou, A. Du, J. van Kasteren and Y. Wang, *Mater. Lett.*, 2009, **63**, 1851–1854.

33 A. Pinkert, K. N. Marsh, S. Pang and M. P. Staiger, *Chem. Rev.*, 2009, **109**, 6712–6728.

34 H. Mussana, X. Yang, M. Tessima, F. Han, N. Iqbal and L. Liu, *Ind. Crops Prod.*, 2018, **113**, 225–233.

35 R. Gavillon and T. Budtova, *Biomacromolecules*, 2008, **9**, 269–277.

36 S. T. Nguyen, J. Feng, N. T. Le, A. T. T. Le, N. Hoang, V. B. C. Tan and H. M. Duong, *Ind. Eng. Chem. Res.*, 2013, **52**, 18386–18391.

37 B. Xiong, P. Zhao, K. Hu, L. Zhang and G. Cheng, *Cellulose*, 2014, **21**, 1183–1192.

38 M. Isik, H. Sardon and D. Mecerreyes, *Int. J. Mol. Sci.*, 2014, **15**, 11922–11940.

39 A. Isogai and R. H. Atalla, *Cellulose*, 1998, **5**, 309–319.

40 N. H. N. Do, T. P. Luu, Q. B. Thai, D. K. Le, N. D. Q. Chau, S. T. Nguyen, P. K. Le, N. Phan-Thien and H. M. Duong, *Mater. Technol.*, 2020, **35**, 807–814.

41 X. Zhang, L. P. Kwek, D. K. Le, M. S. Tan and H. M. Duong, *Polymers*, 2019, **11**, 1942.

42 Y. Li, N. Grishkewich, L. Liu, C. Wang, K. C. Tam, S. Liu, Z. Mao and X. Sui, *Chem. Eng. J.*, 2019, **366**, 531–538.

43 S. Xiao, R. Gao, Y. Lu, J. Li and Q. Sun, *Carbohydr. Polym.*, 2015, **119**, 202–209.

44 J. Cai, S. Kimura, M. Wada, S. Kuga and L. Zhang, *ChemSusChem*, 2008, **1**, 149–154.

45 L. Qian, M. Yang, H. Chen, Y. Xu, S. Zhang, Q. Zhou, B. He, Y. Bai and W. Song, *Carbohydr. Polym.*, 2019, **218**, 154–162.

46 M. Rostamitabar, G. Seide, S. Jockenhoevel and S. Ghazanfari, *Appl. Sci.*, 2021, **11**, 1525.

47 G. Zhu, H. Xu, A. Dufresne and N. Lin, *ACS Sustain. Chem. Eng.*, 2018, **6**, 7168–7180.

48 V. Rahmanian, T. Pirzada, S. Wang and S. A. Khan, *Adv. Mater.*, 2021, **33**, 2102892.

49 A. Song, Y. Huang, B. Liu, H. Cao, X. Zhong, Y. Lin, M. Wang, X. Li and W. Zhong, *Electrochim. Acta*, 2017, **247**, 505–515.

50 F. Chen, M. Xu, L. Wang and J. Li, *BioResources*, 2011, **6**, 1262–1272.

51 B. S. Yang, K.-Y. Kang and M.-J. Jeong, *J. Korean Phys. Soc.*, 2017, **71**, 478–482.

52 G. Aufischer, B. Kamm and C. Paulik, *Int. J. Biobased Plast.*, 2021, **3**, 19–28.

53 H. Bian, Y. Gao, R. Wang, Z. Liu, W. Wu and H. Dai, *Cellulose*, 2018, **25**, 1309–1318.

54 K. S. Mikkonen, K. Parikka, A. Ghafar and M. Tenkanen, *Trends Food Sci. Technol.*, 2013, **34**, 124–136.

55 D. T. Tran, S. T. Nguyen, N. D. Do, N. N. T. Thai, Q. B. Thai, H. K. P. Huynh, V. T. T. Nguyen and A. N. Phan, *Mater. Chem. Phys.*, 2020, **253**, 123363.

56 N. A. Azahari, A. Othman and H. Ismail, *J. Phys. Sci.*, 2011, **22**, 15–31.

57 C. Jin, S. Han, J. Li and Q. Sun, *Carbohydr. Polym.*, 2015, **123**, 150–156.

58 J. Li, Y. Lu, D. Yang, Q. Sun, Y. Liu and H. Zhao, *Biomacromolecules*, 2011, **12**, 1860–1867.

59 Y. Liao, Z. Pang and X. Pan, *ACS Sustain. Chem. Eng.*, 2019, **7**, 17723–17736.

60 J. Xia, Z. Liu, Y. Chen, Y. Cao and Z. Wang, *Cellulose*, 2020, **27**, 879–894.

61 X. Yue, T. Zhang, D. Yang, F. Qiu and Z. Li, *J. Clean. Prod.*, 2018, **199**, 411–419.

62 J. W. Loh, X. Y. Goh, P. T. T. Nguyen, Q. B. Thai, Z. Y. Ong and H. M. Duong, *J. Polym. Environ.*, 2022, **30**, 681–694.

63 Q. Ba Thai, T. Ee Siang, D. Khac Le, W. A. Shah, N. Phan-Thien and H. M. Duong, *Colloids Surf., A*, 2019, **577**, 702–708.

64 Q. B. Thai, R. O. Chong, P. T. T. Nguyen, D. K. Le, P. K. Le, N. Phan-Thien and H. M. Duong, *J. Environ. Chem. Eng.*, 2020, **8**, 104279.

65 Q. B. Thai, D. K. Le, N. H. N. Do, P. K. Le, N. Phan-Thien, C. Y. Wee and H. M. Duong, *J. Environ. Chem. Eng.*, 2020, **8**, 104016.

66 H. Koh, D. Le, G. Ng, X. Zhang, N. Phan-Thien, U. Kureemun and H. Duong, *Gels*, 2018, **4**, 43.

67 D. K. Le, G. N. Ng, H. W. Koh, X. Zhang, Q. B. Thai, N. Phan-Thien and H. M. Duong, *Mater. Chem. Phys.*, 2020, **239**, 122064.

68 B. J. Y. Yam, D. K. Le, N. H. Do, P. T. T. Nguyen, Q. B. Thai, N. Phan-Thien and H. M. Duong, *J. Environ. Chem. Eng.*, 2020, **8**, 104101.

69 M.-H. Du, Q. Wei, Z.-R. Nie, S.-P. Cui, S.-W. Liu and Q.-Y. Li, *J. Sol-Gel Sci. Technol.*, 2017, **81**, 427–435.

70 P. Zhu, M. Zheng, S. Zhao, J. Wu and H. Xu, *J. Wuhan Univ. Technol. Sci. Ed.*, 2015, **30**, 908–913.

This journal is © The Royal Society of Chemistry 2022

J. Mater. Chem. A, 2022, **10**, 23467–23482 | **23481**

71 A. Kayvani Fard, G. Mckay, Y. Manawi, Z. Malaibari and M. A. Hussien, *Chemosphere*, 2016, **164**, 142–155.

72 B. Li, X. Liu, X. Zhang, J. Zou, W. Chai and Y. Lou, *J. Chem. Technol. Biotechnol.*, 2015, **90**, 2106–2112.

73 Y. He, Y. Liu, T. Wu, J. Ma, X. Wang, Q. Gong, W. Kong, F. Xing, Y. Liu and J. Gao, *J. Hazard. Mater.*, 2013, **260**, 796–805.

74 K. Uetani and K. Hatori, *Sci. Technol. Adv. Mater.*, 2017, **18**, 877–892.

75 W. Chen, Q. Li, Y. Wang, X. Yi, J. Zeng, H. Yu, Y. Liu and J. Li, *ChemSusChem*, 2014, **7**, 154–161.

76 L. Heath and W. Thielemans, *Green Chem.*, 2010, **12**, 1448.

77 S.-F. Chin, F. B. Jimmy and S.-C. Pang, *J. Phys. Sci.*, 2016, **27**, 159–168.

78 K. Xie, H. Tu, Z. Dou, D. Liu, K. Wu, Y. Liu, F. Chen, L. Zhang and Q. Fu, *Polymer*, 2021, **215**, 123379.

79 P. Gupta, B. Singh, A. K. Agrawal and P. K. Maji, *Mater. Des.*, 2018, **158**, 224–236.

80 H. Sehaqui, M. Salajková, Q. Zhou and L. A. Berglund, *Soft Matter*, 2010, **6**, 1824.

81 N. Buchtová and T. Budtova, *Cellulose*, 2016, **23**, 2585–2595.

82 K. Ganesan, A. Dennstedt, A. Barowski and L. Ratke, *Mater. Des.*, 2016, **92**, 345–355.

83 M. Pääkkö, J. Vapaavuori, R. Silvennoinen, H. Kosonen, M. Ankerfors, T. Lindström, L. A. Berglund and O. Ikkala, *Soft Matter*, 2008, **4**, 2492.

84 T. Paulauskiene, A. Teresiute, J. Uebe and A. Tadzijevas, *J. Mar. Sci. Eng.*, 2022, **10**, 491.

85 Z.-Y. Wu, C. Li, H.-W. Liang, J.-F. Chen and S.-H. Yu, *Angew. Chem., Int. Ed.*, 2013, **52**, 2925–2929.

86 P. Huang, P. Zhang, L. Min, J. Tang and H. Sun, *Bioresour. Technol.*, 2020, **315**, 123815.

87 D. A. S. Agostinho, A. I. Paninho, T. Cordeiro, A. V. M. Nunes, I. M. Fonseca, C. Pereira, A. Matias and M. G. Ventura, *Mater. Chem. Phys.*, 2020, **253**, 123290.

88 S. Erakovic, A. Jankovic, G. Tsui, C.-Y. Tang, V. Miskovic-Stankovic and T. Stevanovic, *Int. J. Mol. Sci.*, 2014, **15**, 12294–12322.

89 D. Fairén-Jiménez, F. Carrasco-Marín and C. Moreno-Castilla, *Carbon*, 2006, **44**, 2301–2307.

90 E. Guilminot, F. Fischer, M. Chatenet, A. Rigacci, S. Berthon-Fabry, P. Achard and E. Chainet, *J. Power Sources*, 2007, **166**, 104–111.

91 P. Mäki-Arvela, I. Anugwom, P. Virtanen, R. Sjöholm and J. P. Mikkola, *Ind. Crops Prod.*, 2010, **32**, 175–201.

92 H. Abushammala and J. Mao, *Polymers*, 2020, **12**, 195.

93 S. Hazarika, N. N. Dutta and P. G. Rao, *Sep. Purif. Technol.*, 2012, **97**, 123–129.

94 J. Sun, J. Shi, N. V. S. N. Murthy Konda, D. Campos, D. Liu, S. Nemser, J. Shamshina, T. Dutta, P. Berton, G. Gurau, R. D. Rogers, B. A. Simmons and S. Singh, *Biotechnol. Biofuels*, 2017, **10**, 154.

95 L. D. Gelb, in *Aerogels Handbook*, Springer New York, New York, NY, 2011, pp. 565–581.

96 R. Chandrasekaran, M. Hillgärtner, K. Ganesan, B. Milow, M. Itskov and A. Rege, *Sci. Rep.*, 2021, **11**, 10198.

97 A. Rege, M. Schestakow, I. Karadagli, L. Ratke and M. Itskov, *Soft Matter*, 2016, **12**, 7079–7088.

98 M. Dosta, K. Jarolin and P. Gurikov, *Molecules*, 2019, **24**, 2543.

23482 | *J. Mater. Chem. A*, 2022, **10**, 23467–23482

This journal is © The Royal Society of Chemistry 2022